Geography and Sustainability 1 (2020) 304–316

Contents lists available at ScienceDirect

Geography and Sustainability

journal homepage: www.elsevier.com/locate/geosus

Article

Complex causes and consequences of rangeland greening in South America – multiple interacting natural and anthropogenic drivers and simultaneous ecosystem degradation and recovery trends

Wang Li[a,b,c,*], Robert Buitenwerf[a,b], Renata Nicora Chequín[d], Javier Elias Florentín[d], Roberto Manuel Salas[d], Julia Carolina Mata[a,b], Li Wang[c], Zheng Niu[c,e], Jens-Christian Svenning[a,b]

[a] Center for Biodiversity Dynamics in a Changing World (BIOCHANGE), Aarhus University, Ny Munkegade 114, Aarhus C 8000, Denmark
[b] Section for Ecoinformatics and Biodiversity, Department of Biology, Aarhus University, Ny Munkegade 114, Aarhus C 8000, Denmark
[c] State Key Laboratory of Remote Sensing Science, Aerospace Information Research Institute, Chinese Academy of Sciences, Beijing 100101, China
[d] Instituto de Botánica del Nordeste (CONICET-UNNE), Sargento Cabral 2131, c.c. 209, C.P. 3400, Argentina
[e] University of Chinese Academy of Sciences, Beijing 100049, China

HIGHLIGHTS

- The Iberá rangeland showed overall net greening but also substantial local browning.
- Rangeland greening is linked to land use, surface water changes, fire, and climate.
- Fire tended to reduce the greening both in protected and unprotected areas.
- Woody expansion driven by tree plantations occurred mainly in unprotected land.
- Overall greening resulted from multiple trends has a negative impact on biodiversity.

GRAPHICAL ABSTRACT

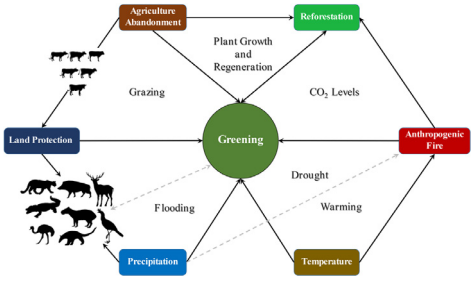

ARTICLE INFO

Article history:
Received 8 October 2020
Received in revised form 14 December 2020
Accepted 14 December 2020
Available online 18 December 2020

Keywords:
South America
Rangeland
Vegetation greening
Climate change
Sustainability
Remote sensing

ABSTRACT

Land-surface greening has been reported globally over the past decades. While often seen to represent ecosystem recovery, the impacts on biodiversity and society can also be negative. Greening has been widely reported from rangelands, where drivers and processes are complex due to its high environmental heterogeneity and societal dynamics. Here, we assess the complexity behind greening and assess its links to various drivers in an iconic, heterogeneous rangeland area, the Iberá Wetlands and surroundings, in Argentina. Time-series satellite imagery over the past 19 years showed overall net greening, but also substantial local browning both in protected and unprotected areas, linking to land use, temporal changes in surface water, fire, and weather. We found substantial woody expansion mainly in the unprotected land, with 37% contributed by tree plantations and the remaining 63% by spontaneous woody expansion, along with widespread transitions from terrestrial land to seasonal surface water. Fire occurrences tended to reduce greening with unprotected areas experiencing widespread and frequent fire. However, protected areas had more browning in unburnt areas than burned areas. Temporal variation in annual precipitation and temperature tended to nonlinearly influence fire occurrences with an interplay of human fire management, further shaping the vegetation greening, pointing to high complexity behind the observed rangeland greening involving interactions among local drivers. Our findings highlight that the observed overall greening is an outcome of multiple trends with clear negative impacts on biodiversity and the local livestock-oriented culture (notably expanding tree plantations) and spontaneous vegetation dynamics, partly involving

* Corresponding author: Tel: +45 52688280; Fax: +45 87154326.
E-mail address: lwwhdz@sina.com (W. Li).

https://doi.org/10.1016/j.geosus.2020.12.002

spontaneous woody expansion. The latter has positive potential for biodiversity and ecosystem services in terms of woodland recovery, but can become negative in such a natural savanna region if expansions develop on a too broad scale, highlighting the importance of ensuring recovery of natural fire and herbivory regimes in protected areas along with sustainable rangeland management elsewhere.

1. Introduction

Global land surface greening has been observed by long-term remote sensing satellites over the past four decades, indicating statistically significant increases in greening leaves over time (Macias-Fauria et al., 2012; Zhu et al., 2016; Chen et al., 2019; Myers-Smith et al., 2020; Piao et al., 2020). Such greening areas occupied about one-third of global vegetated areas by the year 2017 (Chen et al., 2019). A large proportion of the global greening is contributed by tree plantations and cropland from China and India, highlighting the important role of human land-use practices (i.e., fertilization, irrigation, forestry, and grazing) in shaping the land surface dynamics (Malhi et al., 2008; Chen et al., 2019; Piao et al., 2020). Meanwhile, the arctic tundra, African rangeland savanna, Himalayan forests, and European semi-natural vegetated areas also experienced significant greening, often through spontaneous woody expansion with land abandonment and climate change as important drivers (Macias-Fauria et al., 2012; Vickers et al., 2016; Mishra and Mainali, 2017; Buitenwerf et al., 2018; Conradi, 2018; Myers-Smith et al., 2020; Venter et al., 2018). In addition, both empirical models and dynamic global vegetation models have showed that biogeochemical drivers such as fertilization effects from elevated atmospheric CO_2 and nitrogen deposition, are also potentially important drivers of global vegetation greening (Piao et al., 2015; Zhu et al., 2016; Mishra and Mainali, 2017). The global greening trend is likely to alter the global terrestrial water cycle, soil carbon storage, and the surface energy budget (Pearson et al., 2013; Piao et al., 2015; Forkel et al., 2016). Disentangling the complexity behind the global greening trend is crucial for our understanding of global change and therefore facilitates how we approach sustainable ecosystem restoration (Hegerl et al., 2010).

As the most common ice-free form of the land surface on Earth (Fuhlendorf and Engle, 2001; Godde et al., 2018), rangelands significantly contribute to the global vegetation greening (Archer et al., 2017). Rangelands are grasslands, shrublands, open woodlands, or other vegetation, often highly heterogeneous, grazed by livestock or wild herbivores (Archer et al., 2017). Woody expansion in rangelands displaces herbaceous grass cover and has been widely identified in Africa, South America, and Australia (Lunt et al., 2010; González-Roglich et al., 2015; Stevens et al., 2016b; Devine et al., 2017; Li et al., 2020b), contrasting with deforestation and dieback occurring in many forested areas (Archer et al., 2017). The woody expansion in rangelands has been driven by different social-ecological and climatic factors including the elevated atmospheric CO_2 (Bond and Midgley, 2000; Buitenwerf et al., 2012), climate change (e.g., rainfall patterns) (Kulmatiski and Beard, 2013; Brandt et al., 2017; Venter et al., 2018; Zhang et al., 2019), changes in fire regimes and livestock management (e.g., overgrazing) (Daskin et al., 2016; Stevens et al., 2016a), as well as land use management changes (e.g., land protection) (O'Connor et al., 2014) (Fig. 1). The interactions among these factors and the associated ecosystem activities (e.g., grazing, land cover transition, climate events) are likely to increase the uncertainty and complexity behind the rangeland greening (Fig. 1). There is widespread concern that woody expansion is likely to reduce rangeland carrying capacities for wild and domestic large grazers (Archer et al., 2017; Venter et al., 2018), have negative effects on biodiversity (Bond and Parr, 2010), and may further affect ecosystem functioning (e.g., fire regimes).

Compared to the drivers of deforestation, the drivers of woody expansion in rangelands and their interactions are complex and poorly understood (Venter et al., 2018), due to the highly heterogeneous vegetation structure (e.g., stature and density) and functioning (e.g., biomass) alongside multiple ecosystem types and land uses. High variation in composition, productivity, and diversity across different scales make many rangelands inherently heterogeneous (Patten and Ellis, 1995; Fuhlendorf and Smeins, 1999; Fuhlendorf and Engle, 2001). The high heterogeneity of rangelands makes it complicated to identify the driving mechanisms behind greening pattern in rangelands. Notably, the complex interplay between climate, land use, and fire are not well understood, making it more difficult to design future management.

Apart from the management of rangelands for livestock production, rangelands support a range of other uses, hereunder uses that convert rangelands to other land cover categories, e.g., cropland (Tsegaye et al., 2010; Li et al., 2020a). A rising threat to rangelands comes from afforestation, where tree plantations are being established in rangeland areas for commercial wood production or various perceived ecosystem services such as erosion control or climate mitigation. For instance, about 3.5 million km^2 grass-dominated areas in Africa have been targeted to restore forest landscapes by 2030 (www.bonnchallenge.org). Widespread planting of exotic eucalypt and pine monocultures in savannas occurs in many regions, e.g. Brazil, Colombia, Nigeria, and Congo (Fernandes et al., 2016). Such afforestation is highly negative for rangeland biodiversity, and the ecosystem services provided are often questionable (Veldman et al., 2015; Fernandes et al., 2016; Bond et al., 2019; Fagan, 2020).

In summary, landscapes in the real world are heterogeneous, resulting in potentially high complexity behind general greening trends in global and local ecosystem contexts. Understanding this complexity is central to assessing the implications, notably the extent to which greening represents ecosystem recovery or, rather, increased human-driven pressures and loss of semi-natural habitats. To address this issue, we use satellite imagery from the past 19 years (2000—2018) to quantify the rate of greenness change and relate the preceding greening trends with the up-to-date land cover status and multiple anthropogenic and climatic factors in the Iberá Wetland region (hereafter, Iberá) in Argentina. Iberá offers an excellent model for studying this complexity due to its high heterogeneous environments and land uses. We ask the following specific questions: 1) Is Iberá greening like many other rangelands across the world? 2) What are the underlying land cover transitions? 3) How are these dynamics related to potential drivers – inter-annual weather variation, fire regimes, dam construction, afforestation, and natural areas' recovery through declining land-use intensity and expansion of protected areas? Notably, we hypothesized that the vegetation greening in Iberá includes a major component driven by expanding tree plantations and also is affected by hydrological dynamics linked to hydrological effects of the Yacyretá Dam, i.e., human-driven environmental changes with problematic consequences for biodiversity and ecosystem services in the region. We furthermore expect that greening trends will be modulated by inter-annual weather variation and fire regimes, as is typically seen in rangelands (Durigan and Ratter, 2016; Beckage et al., 2019), and differing degrees of conservation protection, with increased greening under reduced drought stress, reduced fire, and increased protection. 4) What are the implications for interpreting global greening trends and for rangeland management?

2. Materials and Methods

2.1. Study site

The Iberá Wetlands and surroundings in Corrientes in northern Argentina (Fig. 2) represents a typically complex rangeland landscape. The

dominate ecosystem type is rangeland, but the landscape harbours high heterogeneity in land protection levels, from fully protected nature reserves (Iberá Natural Reserve, Mburucuyá National Park, and Socorro, Fig. 2f-g) to unprotected rangelands and commercial forestry, and in ecosystem structure, with a mix of dry and temporarily flooded grasslands, savanna and shrubland, woodland, as well as marshes, lagoons and rivers (Zamboni et al., 2017). Outside Iberá Natural Reserve, tree plantations, cattle raising, and agriculture crop cultivation are important land use purposes, generating crucial economic incomes to the local people. Tree plantations have increasingly replaced cattle farming and grasslands, with negative impacts on the traditional livestock-oriented culture and local native biodiversity (Holl and Brancalion, 2020). Crop cultivation (e.g. rice) also highly affects the ecosystem structure, directly through the vegetation change, but also through the hydraulic systematization of the terrain to favor flooding, periodic movement of soil, and the extraction of water from the lagoons for cultivation (Neiff and de Neiff, 2006).

The Iberá Wetland (Esteros del Iberá) is an important component of this region, as a very large (~1400 km^2) freshwater wetland area and strongly affected by the nearby Yacyretá Dam, a large hydroelectric power plant on the Paraná River. The wetlands differentiate Iberá from many other rangelands in the world, playing an important role in the rangeland ecosystem functioning (i.e., carbon and water cycle, soil decomposition) and providing crucial habitats to aquatic plants and animals (Canziani et al., 2006). The terrain is very flat with the water flowing slowly through the region (Montroull et al., 2013). Fluctuations in the water surface, in the permanent and seasonal water body, and the wetlands, as well as the transitions among these water-related surfaces and the terrestrial surface, are likely to influence the satellite observed vegetation dynamics (Stow et al., 2004). However, the close linkages between aquatic and terrestrial environments with permanent and temporary inundation make it challenging to disentangle how anthropogenic and natural environmental factors shape the rangeland dynamics. Together with climate change, dam construction has caused a substantial increase in the water level in the Iberá rangeland ecosystem since 1989, resulting in losses of thousands of hectares of productive lands at the early stage (Blanco et al., 2003; Canziani et al., 2006).

Historically, the Iberá region suffered strong defaunation, but in the last decades, active restoration of the fauna has begun through increased protection and direct reintroductions (Zamboni et al., 2017). Importantly, the core area of Iberá has been declared a national park (1,381.4 km^2) since 2016 (Zamboni et al., 2017). Meanwhile, livestock grazing and crop farming have been significantly reduced within the natural reserve after the region became protected and the surface water expansion that was caused by the Yacyretá Dam construction (Bauni et al., 2015). The increased protection and active restoration are likely to affect the vegetation dynamics in the region.

2.2. Land surface greening and browning trends

Time series of annual 250-m NDVI means ($\overline{NDVI}$) between 2000 and 2018 were used to quantify land surface greenness change over time, considering its higher and more consistent data availability than other satellite products e.g., Landsat (Li et al., 2020a). The temporal trend analysis was conducted based on the annual mean MODIS NDVI collection (MOD13Q1, 250 m, 16-day interval) using the Mann-Kendall (MK) test of monotonic change (Mann, 1945). As a useful alternative to linear squares regression with low assumptions, the MK test is a rank-based non-parametric test (Eddy et al., 2017), and is easy to calculate, robust against non-normality as well as less sensitive to missing values and outliers (de Jong et al., 2011; Wang et al., 2020). In this study, the Sen's slope for time series $\overline{NDVI}$ was used to represent the vegetation greening rate (hereafter, GR, yr^{-1}, with negative values representing browning rate), considered to be a good approximation to evaluate the net change throughout the studied time range. In this study, we set the significance level to $p < 0.05$ when using the non-parametric Mann-Kendall test to quantify greening and browning as statistically significant increasing and decreasing trends in $\overline{NDVI}$. Only pixels with statistically significant trend were used in the analysis.

2.3. Land cover transition and mapping

Considering the data availability, we quantified the long-term land cover transition based on broad-scale land cover products between 2001 and 2018 and re-mapped the up-to-date land cover types in 2018 with the combined use of different satellite products at a fine scale (Fig. S1).

Long-term land cover transition

Broad-scale (500 m) land cover changes were mapped using a time series of MODIS land cover product (MCD12Q1 V6, http://LPDAAC.usgs.gov). A per-pixel land cover transition matrix was calculated to quantify transitions between the main land cover types between 2001 and 2018 using the software Dinamica EGO (Soares-Filho et al., 2009). The main land cover types include evergreen needleleaf forests, evergreen broadleaf forests, deciduous broadleaf forests, woody savannas, savannas, grassland, permanent wetlands, croplands, urban and built-up lands, barren, water bodies (Table S1, Fig. S2). The 500-m map was reclassified before the calculation of land cover transition matrix by merging all forest classes and woody savannas into a woodland class.

Long-term surface water cover transition

Fine-scale (30 m) surface water changes were mapped using the Landsat global surface water product (Pekel et al., 2016). Reclassification was conducted by classifying the land cover into three main types (terrestrial land, permanent water, seasonal water) in the year 1985 (shortly after the construction of Yacyretá Dam in 1983) and 2018 according to the definition of each surface water transition type (Table S2) (Pekel et al., 2016). The reclassification of surface water aimed to capture seasonal dynamics in water coverage, which is important in this wetland setting, where seasonal surface water generates various vegetation types, and its seasonal changes could influence greening trends. A per-pixel transition matrix was calculated to quantify transitions between land and surface water between 1985 and 2018. According to the yearly historical layer of surface water, we counted the area of permanent and seasonal water for each year from 2000 and 2018 to describe the surface water's temporal patterns.

Latest fine-scale land cover mapping

The Copernicus Dynamic Land Cover (CGLS-LC100) product (100 m) in 2015 was used as the basic map of the latest land cover distribution (Buchhorn et al., 2019). Compared to the coarse-scale MODIS land cover map, the CGLS-LC100 land cover map was produced based on a relatively detailed classification system but with a shorter time span (Buchhorn et al., 2019). One obvious difference is that the CGLS-LC100 further differentiates the grassland and woody cover (including shrubland and forests) from the broad-scale savanna class in the MODIS product (Table S1). In order to differentiate the natural forests from tree plantations, we extracted all the forest cover types from the CGLS-LC100 map as a mask layer of the forest class. Then, the forest mask layer was used to extract forest areas from the MODIS NDVI time series between 2000 and 2018. Convolution neural network classification with an overall accuracy of 89% was conducted based on the time-series MODIS NDVI pixels by classifying the forest pixels to natural forest and planted forest. Due to large patches of homogeneous forest pixels existing in the study site, we selected at least 2000 sample pixels for each forest type across the study area assisted by the field photographs and historical high spatial resolution imagery from Google Earth. The selected pixels were randomly divided into 80% for model training and 20% for independent validation. This classification was further validated using expert knowledge of the three co-authors who possess intensive knowledge of the study site. Based on visual interpretation, tree

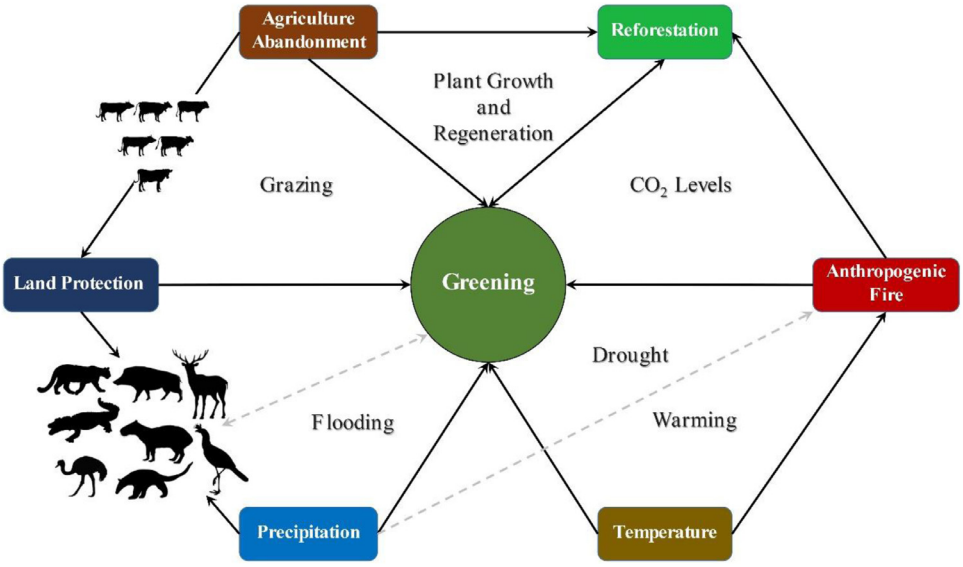

Fig. 1. Conceptual diagram showing the complex interactions among different social-ecological and climatic factors potentially shaping vegetation greening in rangeland ecosystems. The key words in the boxes represent typical drivers of ecosystem change in rangelands, with the words between the arrows indicating the resulting proximate mechanisms of change. The arrows represent interaction among environmental factors (e.g., spontaneous reforestation might happen after agriculture abandonment and contributes to vegetation greening). The grey dashed lines represent potential interactions. The animal pictograms in the left corner represent the wild fauna of the Iberá Wetland area, some of which have been re-introduced to protected areas in the region by the Rewilding Argentina as part of restoration efforts.

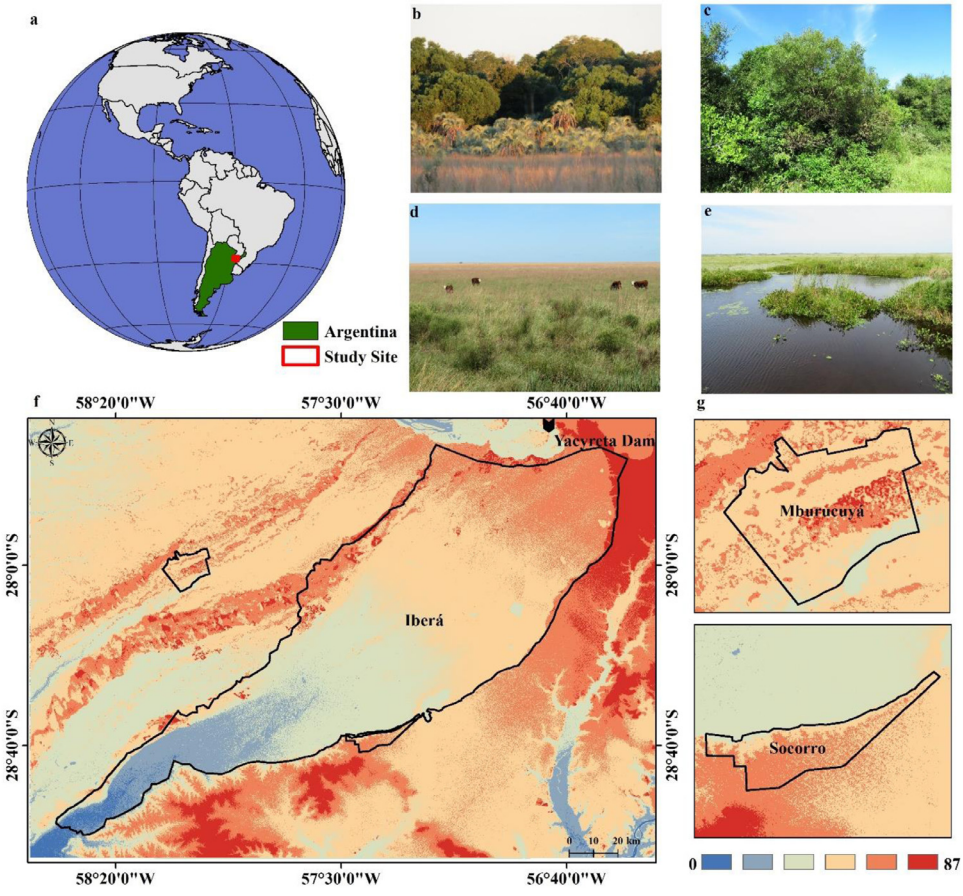

Fig. 2. Study site: (a) Iberá Ecosystem in Argentina, South America. Typical land cover types include (b) Woodland; (c) Shrubland; (d) Dry grassland; and (e) Herbaceous wetland. The study site includes three protected areas, compring the (f) Iberá Natural Reserve (g) Mburucuyá National Park and Socorro. Boundaries of the protected areas are overlaid on a digital elevation model (unit: meter). Photographs were taken by one of the co-authors.

plantations showed a distinctive regular geometry, closed and homogenous canopy texture, as well as time series NDVI profile compared to the natural forests. This imagery feature differences facilitated the automatic differentiation of tree plantations from natural forests. For the surface water types, we merged the seasonal water surface information from the Landsat surface water map into the final land cover map as the up-to-date land cover status in 2018 (**Fig. S3a**). We resampled the 30-m surface water map to 10-m resolution and replaced the pixels of water class from CGLS-LC100 map by two classes provided by the reclassified surface water map, namely, permanent water and seasonal water.

2.4. Ecological response to fire and weather dynamics

The ecological response of vegetation greening to fire and weather dynamics were investigated by linking the MODIS-derived greening data to the environmental factors including fire, precipitation and tempera-

ture. All the environmental factors were re-sampled to a spatial resolution of 250 m in order to be consistent with the MODIS-derived greening data before subsequent analysis.

To assess the ecological response of the vegetation dynamics to fire, we quantified the fire frequency using the MODIS fire product (MCD64A1) by summing the number of fire occurrences for each pixel from 2001 to 2018 (Giglio et al., 2009). The fire frequency (FireFreq) was classified into four levels according to the annual fire occurrences, namely, NoFire (FireFreq = 0), low level (0 < FireFreq < 2), medium level (2 ≤ FireFreq ≤ 6), and high level (FireFreq > 6). The distribution of greening and browning pixels was counted according to different fire frequency levels and protection status [i.e., the proportion of greening pixels in protected areas with high fire frequency = (Number of greening pixels in high fire frequency in protected areas) / (total number of pixels in high fire frequency pixels)].

To assess the ecological response to inter-annual weather variation, the capacity of the ecosystem to maintain greenness under inter-annual variation in rainfall/temperature (i.e., drought stress and heat stress) was quantified by analysing how vegetation greenness (NDVI) responds to annual precipitation, annual mean temperature, and how the NDVI anomaly responds to the anomalies of precipitation and temperature. We interpret this capacity as the resistance component of ecological resilience (Walker et al., 2004; Li et al., 2020a). Generalized linear regression was conducted to fit the relationship between NDVI and climatic factors between 2000 and 2018 by setting a significant level of $p < 0.05$. We quantified the annual mean of total precipitation (MAP) from 2000 to 2018 based on a time series of annual total precipitation observed by the Climate Hazards Group InfraRed Precipitation with Station data (CHIRPS) (Funk et al., 2014). The annual mean temperature (MAT) was quantified based on the time-series of annually composited temperature from the TerraClimate dataset (Abatzoglou et al., 2018). The Mann-Kendall (MK) test was further applied to the time-series of annual precipitation and temperature data to quantify the precipitation change rate (PreRate), and the temperature change rate (TempRate), respectively. The Sen's slope from the MK test was used to represent PreRate and TempRate. A positive PreRate (TempRate) value represents an increase in precipitation (temperature), and a negative PreRate (TempRate) represents a decrease in precipitation (temperature).

We also investigated how vegetation greening responds to the weather trends by correlating the greening rate of four typical vegetation types (woodland, dry grassland, seasonal surface water, and wetland) to PreRate and TempRate. The woodland class was extracted as a union of natural forest, planted forest, and shrubland from the fine-scale land cover map for the year 2018. For each vegetation type, we randomly selected 1000 points for correlation and regression analysis, considering the fact that the subsequent spatial autoregressive analysis is very computation-consuming. We used ordinary least-squares (OLS) regression and simultaneous autoregressive (SAR) models to statistically quantify the spatial relationships of woody vegetation greening rate to the three environmental factors (FireFreq, PreRate, and TempRate), with the standardized greening rate as the response variable and the environmental factors as the explanatory variables. The SAR model was applied to account for spatial autocorrelation, while also quantifying the contributions from different environmental factors (Kissling and Carl, 2008; Sandel and Svenning, 2013). The regression models' standardized coefficients represent the relative influence of the explanatory variables on the greening rate. We fit an error SAR model based on a connectivity matrix with a distance criterion within 30 km that best removed the spatial autocorrelation from the model residuals according to the computed correlograms. The SAR analysis was conducted using the spatial analysis macroecology (SAM) software (Rangel et al., 2010). The significance level of the coefficients for the OLS and SAR models was quantified by the p value.

3. Results

3.1. Land surface greening and browning trends

Like many other areas, Iberá has experienced a general greening trend. The MODIS NDVI time-series between 2000 and 2018 showed that about 31% of the pixels (~13964 km^2) experienced significant trends in Iberá, with 62% of these revealing greening and 38% browning (Fig. 3). Distinct spatial patterns in pixels with significant greening and browning were found both in protected and unprotected areas (Fig. 3 & Fig. 4a), mainly contributed by herbaceous wetland, grassland, and natural forest (Fig. 4b). Spontaneous natural forest greening within the protected areas after agriculture abandonment and cattle removal overweighed anthropogenic afforestation in the unprotected area (Fig. 4c). Conversely, browning also occurred in protected and unprotected areas, especially in dry grassland and wet herbaceous wetland (Fig. 4d). The increase of seasonal water in the herbaceous wetland is the main cause for the satellite-observed browning in the protected areas, while the fire in unprotected grassland is the overall main contributor.

3.2. Land cover transitions

The greening trend is highly associated with land cover transitions. The coarse-scale (500 m) MODIS land cover maps showed that approximately 15% of the entire Iberá (~6855 km^2) experienced land cover transitions in the past 19 years, with a significant loss of savannas that transited to grassland, wetland, and forests (Fig. 5a). The lost savannas were replaced by the obviously increased forest patches, which started from 2004 outside the protected areas and started from 2012 by the western border within the Iberá Natural Reserve (Fig. S2), with 37% contributed by tree plantations and the remaining 63% by spontaneous woody expansion (Fig. S3a). Significant transitions among surface water and terrestrial land were observed between 1985 and 2018 (occupying 8% of the entire region), with the main transition being from terrestrial land to seasonal surface water (Fig. 5b), with an increase of 2537 km^2 observed mainly within the protected areas. The permanent surface water increased by 367 km^2 due to the significant transition from terrestrial land (Fig. 5b). The surface water has become more fluctuating and seasonal with "permanent seasonal" and "ephemeral seasonal" water surface occupying more than half of the total surface water transitions (Fig. S4a). The water occurrence history shows that the permanent water began to stabilize while the seasonal water has been significantly increasing since 2000 (Fig. S4b). However, the increasing trend of seasonal water areas is highly associated with the general increase of precipitation (Fig. S5a).

3.3. Ecological response to fire and weather dynamics

Widespread fire occurrences have been observed across Iberá (Fig. 6a,b). Regardless of land protection, higher proportions of greening areas are associated with lower fire frequency, while higher proportions of browning areas are associated with higher fire frequency (Fig. 6c). For all the fire frequency levels, protected areas showed relatively lower greening and browning proportions. Inside the protected areas, there are more browning in unburnt areas compared to low/medium fire frequency. The burned areas peaked in 2005 and then kept a significant decreasing trend (Fig. S5b). The temporal changes in burned areas showed a nonlinear relationship with climatic factors (Fig. S5c,d).

High inter-annual variation of precipitation and significant increase of annual temperature were observed in Iberá (Fig. 7a,b). Both NDVI and its anomaly were significantly correlated with the annual precipitation and its anomaly throughout the 2000–2018 period (Fig. 7c,e). However, no significant correlations were observed between the annual

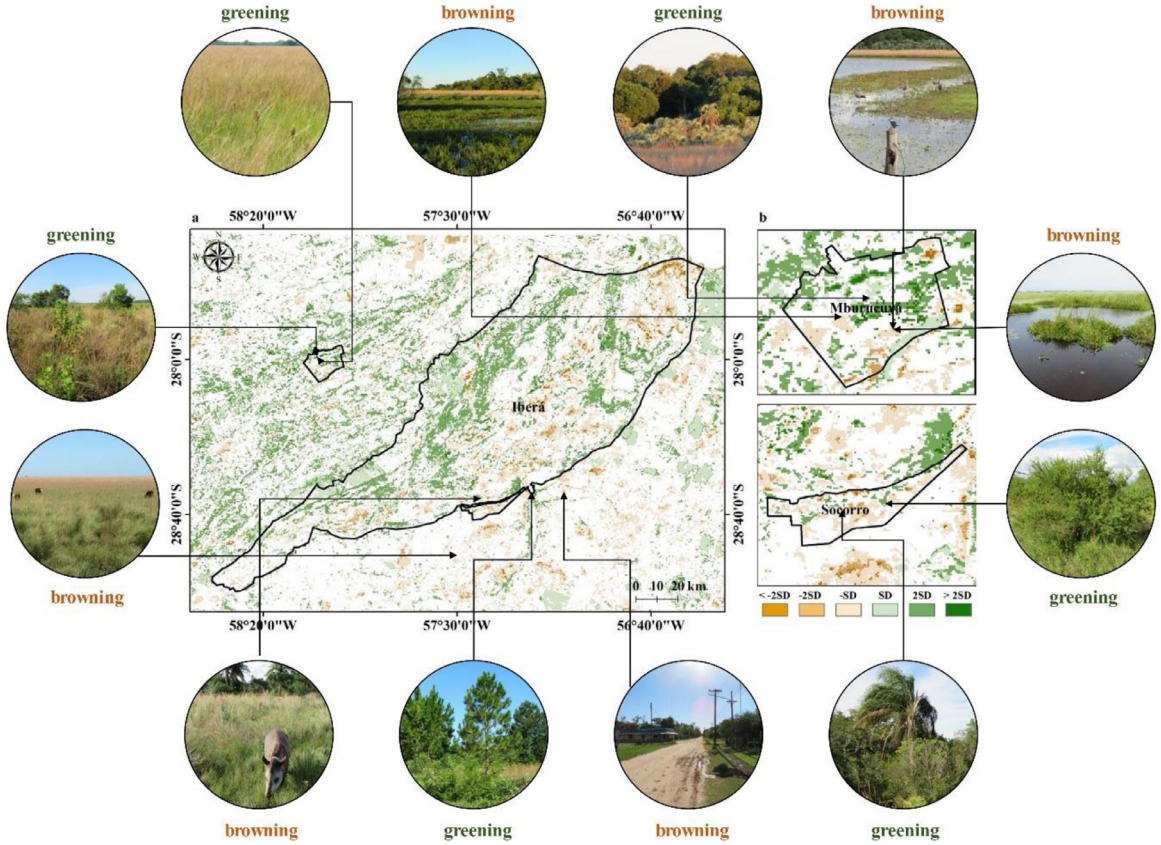

Fig. 3. Temporal vegetation dynamics (greening/ browning) based on NDVI in Iberá. (a) Map of NDVI change rate (yr^{-1}) between 2000 and 2018. NDVI change rates were estimated using the Theil-Sen estimator, a robust estimator of linear change. NDVI change rate maps in protected areas. (b) Zoomed in maps of Mburucuyá National Park and Socorro. Geo-located photographs (taken by one of the co-authors) show the examples of greening and browning spots.

Table. 1
Regressions describing the importance of fire frequency and the weather trends for the greening rate in woodland. Standardized coefficients were derived from ordinary least-squares (OLS) regression model and simultaneous autoregressive (SAR) model. Response variable: woody vegetation greening rate (2000-2018). Explanatory variables: fire frequency (FireFreq), precipitation change rate (PreRate), and temperature change rate (TempRate). R^2 represents variation in coefficients. $^{*}p < 0.05$, $^{**}p < 0.001$.

Independent Variable	Standardized Coefficients	R^2 (N=1000)
Ordinary Least Squares (OLS) Model		
FireFreq	-0.083**	R^2 = 21%; $p < 0.001$
PreRate	0.225*	
TempRate	-0.262**	
Simultaneous Autoregressive (SAR) Model		
FireFreq	-0.064**	R^2 = 38%; $p < 0.001$
PreRate	0.075*	
TempRate	-0.21**	

mean NDVI and temperature, nor their anomalies (Fig. 7d,f) although a more significant increasing trend on temperature was observed (Fig. 7b). Vegetation greening in Iberá was correlated with the weather trends. The greening rate in woodland was positively correlated with precipitation change rate and negatively correlated with temperature change rate, and the opposite relations in the wetland (Fig. 8a,b,e,f). Grassland greening showed no correlation with the weather trends (Fig. 8c,d). A simultaneous autoregressive model (SAR) explained 38% of the spatial pattern of changes in woody vegetation greening rate in terms of fire frequency, change rates in precipitation, and temperature (Table 1). The coefficients of the SAR modeling show that weather variation contributed relatively more to woody greening than fire.

4. Discussion

4.1. Complexity behind land surface greening

Our results showed that more than one-third of Iberá experienced significantly monotonic trends of greenness change. The greening dominated over browning (62% vs 38% of pixels), with the greening/browning patterns related to the heterogeneous land cover and associated transitions. One of the most common land cover changes was the conversion of savannas to grassland, wetland, and forests, with greenness changes associated with transitions to forest and grassy covers. Grassland and herbaceous wetland showed greater dynamics in greening trends than other vegetation types, likely due to their close linkages to the water supply from the seasonal fluctuations in surface water or the inter-annual rainfall changes (Montroull et al., 2013). Significant increases in surface water tended to cause a significant decrease of satellite-observed greenness of herbaceous covers in the protected land, likely reflecting a loss of terrestrial vegetation cover. The increase of permanent surface water is likely or at least partially linked to the construction of the Yacyretá Dam in the northeastern border of the Iberá natural reserve, operating since 1994 (Canziani et al., 2006). Although areas of permanent water, including rivers, lakes, and reservoirs did not change much since 2000, seasonal surface water near permanent water has become more fluctuating, likely linked to climate dynamics and anthropogenic dam infrastructure, illustrating high sensitiveness of wetlands to environmental change (Vörösmarty et al., 2000). The damming is likely to cause a significant loss of terrestrial and riparian plant communities,

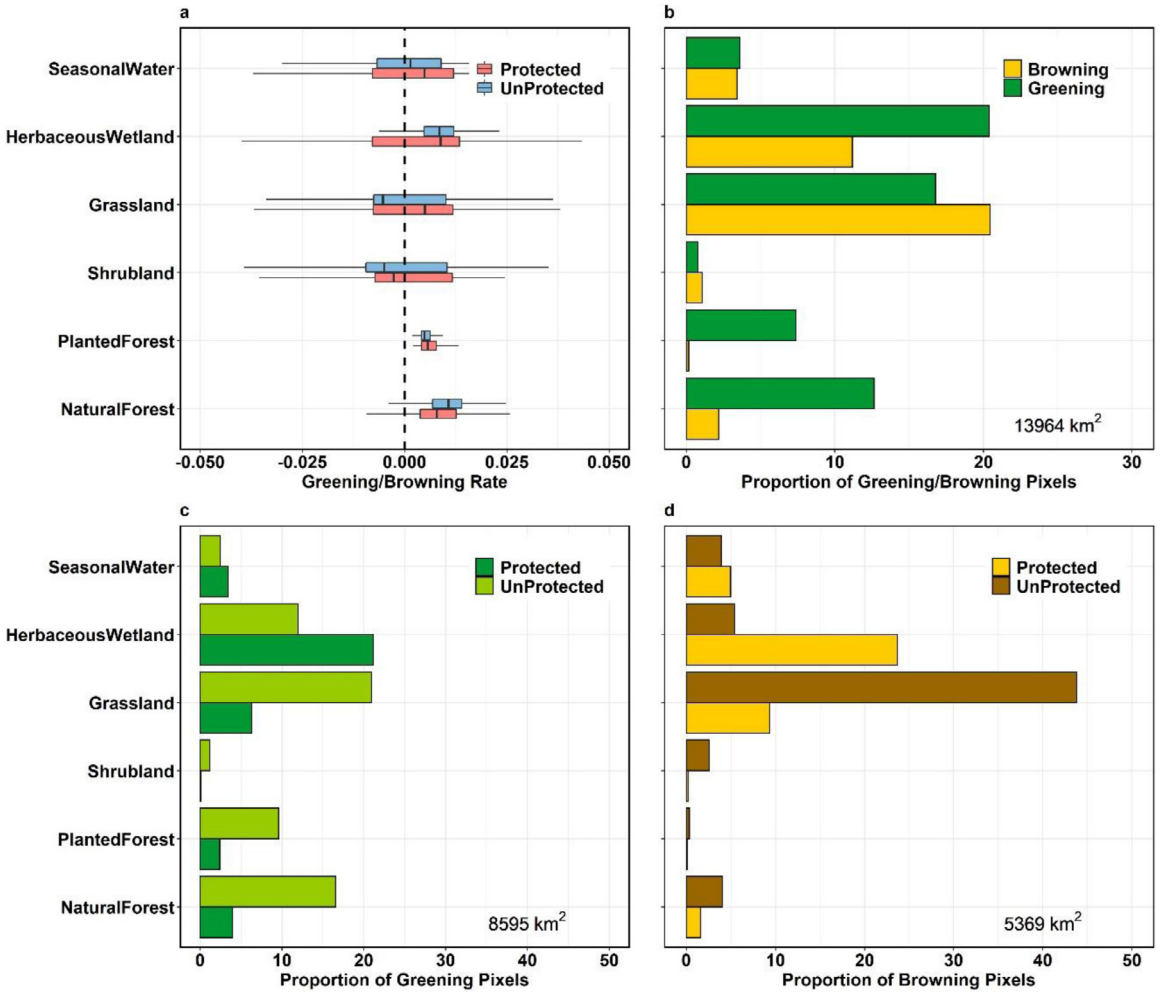

Fig. 4. Greening and browning in vegetation types in Iberá. (a) Boxplot depicts greening and browning pixels within different vegetation types grouped by land protection status (protected and unprotected) for the entire Iberá. (b) Proportions of greening and browning pixels for each vegetation type. (c) Proportions of greening pixels and (d) browning pixels for each vegetation type grouped by land protection.

as it fragmented and transformed water flows in the freshwater Iberá ecosystems (Bauni et al., 2015). Increasing water seasonality may be closely linked to climate dynamics, e.g., more frequent raining seasons caused by El Niño (Holgerson and Raymond, 2016). The increase in surface water has likely affected greening through an inundation-induced decrease of satellite-observed grassy vegetation greenness. For instance, much aquatic vegetation shows increased greenness (seasonal greening) when surface water level is low at dry season, but decreased greenness (seasonal browning) when submerged during the wet season. This illustrates the complexity of factors that may drive greening or browning trends in a complex rangeland landscape.

Our results also showed widespread woody greening in the protected and unprotected areas, associated with industrial tree plantations outside protected areas and spontaneous woody regrowth after land abandonment and cattle removal both inside and outside protected areas (Canziani et al., 2006; González-Roglich et al., 2015). Overgrazing in livestock areas can also cause woody expansion (Anadón et al., 2014), e.g., acacia filled livestock areas at the south border of Iberá (per. obs). The tree plantations tended to form patches with a more homogenous greening rate than the natural forests and other vegetation types, making them more easily identified from the satellite signals across time. Although tree plantations significantly contributed to ecosystem greening, such afforestation is highly negative for biodiversity in savanna ecosystems and negatively affects the functioning of rangelands for livestock production, and hence, it may have negative social effects locally (Veldman et al., 2015; Fernandes et al., 2016; Bond et al., 2019).

Greening from spontaneous woody expansion occurred on a larger scale compared to the greening from tree plantations, but at varying rates. The significant positive/negative correlation between woody greening rate and annual precipitation/temperature variation rate suggests that rapid changes in precipitation and cool climate conditions are likely to intensify woody densification and expansion in Iberá. Such significant correlations provide an important contrary example to recent global-scale study which found no correlation between woody cover change rates and rates of climate change across tundra and savanna biomes (García Criado et al., 2020). The close linkages of climate dynamics to surface water dynamics may also indirectly contribute to woody greening by changing forest hydrological processes, including water supply intercepted by forest canopy and belowground soil absorption (Putuhena and Cordery, 2000; Feng et al., 2016; Zeng et al., 2020). Large-scale tree plantations also require high water supply (e.g., via artificial canals), which may dry up nearby grasslands and wetlands, thereby possibly altering local and regional hydrological cycles (Fernandes et al., 2016). Inter-annual weather variation tended to non-linearly influence fire occurrence (Fig. S5c,d), potentially involving an interplay with fire management (Wei et al., 2020), e.g., fewer fires ignited by people when there are widespread wildfire in warmer years. Such interplays between weather variation and human fire management

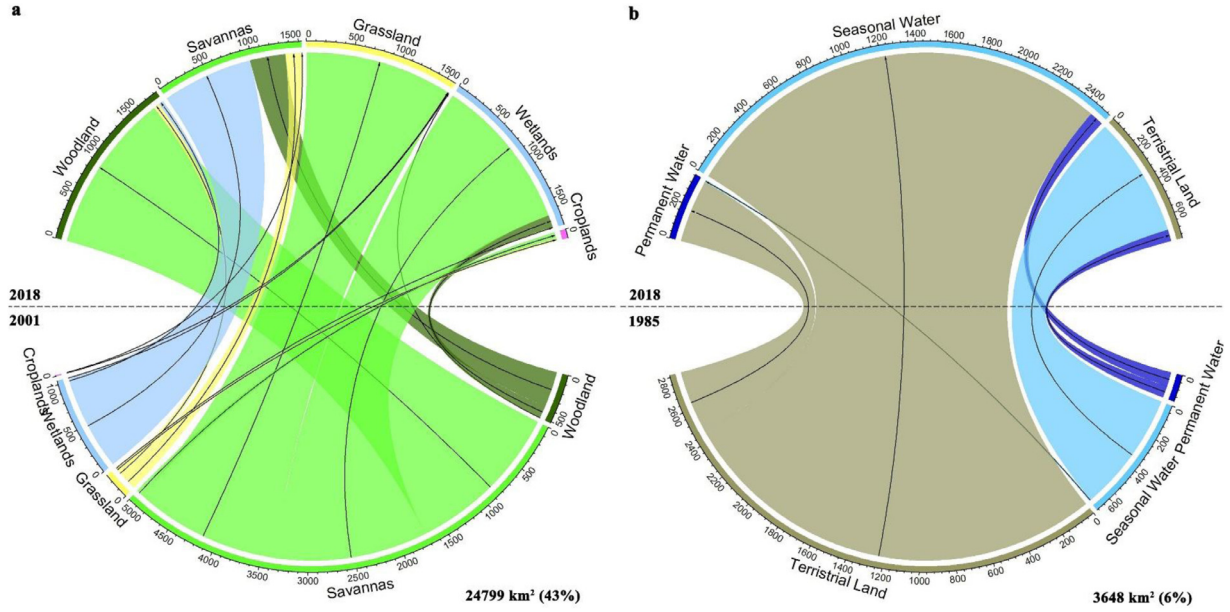

Fig. 5. Land cover transitions in Iberá (a) Transitions among all land cover types observed from coarse-resolution (500 m) MODIS satellite between 2001 and 2018 (considering data availability) shown in Fig. S2. The woodland is a mixture of all types of forests and woody savannas (Table. S1). (b) Transition among water-related surfaces (permanent water, seasonal water) and terrestrial land observed from fine-resolution (30 m) Landsat satellites between 1985 and 2018. The water-related surfaces and land cover transition map was produced by reclassifying the Landsat surface water product (Fig. S3b). The transition matrices were calculated based on the number of pixels converted to the area unit in km^2. The numbers in the ticks represent the area in km^2. The total area of the land cover types in transition is 6855 km^2, occupying 15% of the entire study site. The total area of transitions among water-related surfaces and terrestrial land is 3648 km^2, occupying 8% of the entire study site.

could further shape vegetation greening, pointing to high complexity behind the observed rangeland greening involving interactions among local drivers.

Spontaneous woody expansion to some extent represents an expansion of natural forests and shrubland and therefore has positive effects on biodiversity (Cabral et al., 2003), but if expansions occur broadly across naturally semi-open savanna areas (Bernardi et al., 2016), due to loss of natural herbivory and fire regimes their effects turn negative for biodiversity (Guido et al., 2017). Maintaining high heterogeneity in rangelands will help to promote higher biodiversity, and habitat quality grazed by wildlife and livestock (Fuhlendorf and Engle, 2001; Macias et al., 2014). Hence, land owners should reconsider conventional homogeneity-based rangeland management as it may deteriorate livestock production and sustainability (Holechek et al., 1998; McCollum III et al., 1999).

4.2. Ecological response to land protection, fire and inter-annual weather variation

Our results showed that grassland was the dominant land cover type that showed significant greening and browning regardless of land protection. The most widespread grassland browning was found in unprotected land, suggesting not only great seasonal greenness changes but also potential ecosystem degradation there, likely reflecting high grazing pressure from livestock (Godde et al., 2018; Li et al., 2020a; Li et al., 2020b). High grazing intensity keeps the grass in a short and open mixed with bare ground, leading to reduced greenness. This likely challenge coexistence between livestock and native herbivores through competition for food. The creation of the Iberá Natural Reserve helped reduce cattle grazing pressure and poaching in Iberá (Canziani et al., 2006) and, to some extent, recovered habitats for endangered wildlife, including capybaras (*Hydrochoerus hydrochaeris*), marsh deer (*Blastocerus dichotomus*), and caimans (Zamboni et al., 2017). Grassland greening also occurred in a certain scale across the study site both in the protected and unprotected areas, providing promising feedback to the call for sustainable livestock management practices that aimed to be conducted in Iberá.

In addition to livestock grazing pressure, grassland greening and browning were also linked to fire, partly reflecting fire as an important natural process in Iberá, but even more so active use of fire in rangeland management in both unprotected and protected areas, like many other rangelands across the world. The Iberá Natural Reserve and its surrounding areas were historical livestock areas where fire has been used as a common practice to manage pastures. Ranchers, for example, use fire to promote growth of new grass for livestock consumption, as rangeland vegetation often to a large extent is composed of grasses that become more unpalatable with size and age (e.g., *Coleataenia prionitis*), and production of new leaves after fire favours the livestock (pers. obs.). Thus, frequent fire is likely to result in vegetation browning by causing a sudden loss of photosynthetic foliage (Myers-Smith et al., 2020; Piao et al., 2020). Fire in the unprotected areas is ignited to keep the grass short as livestock prefer higher nutrient concentrations in short, repeatedly grazed grass (Bhola et al., 2012). Fire occurrences showed significant contribution to the vegetation greening in Iberá by removing biomass including a significantly negative contribution to the woody greening (Table 1).

Unlike fire in unprotected areas, fire in the protected areas is ignited to protect the rangelands from the invasion of shrubs, and the accumulation of flammable biomass that could cause wildfires (pers. obs.) (Fig. 6a). However, recurring fires may also decrease habitat quality for wildlife (Durigan and Ratter, 2016; Abreu et al., 2017). For the protected areas, fire management is often considered as a necessary management tool (Kunst, 2011), although the role of fire relative to other factors such as grazing and browsing by wild herbivores under natural conditions is often not well understood due to centuries' of burning and defaunation. The satellite observations showed that burned areas decreased in Iberá since 2005, likely reflecting anthropogenic fire management in the region (i.e., a provincial law on fire management approved in 2006, Prov. Law 5590), and also reduced fire in protected areas compared to when they were formerly used for livestock. Further, the increase of flooded

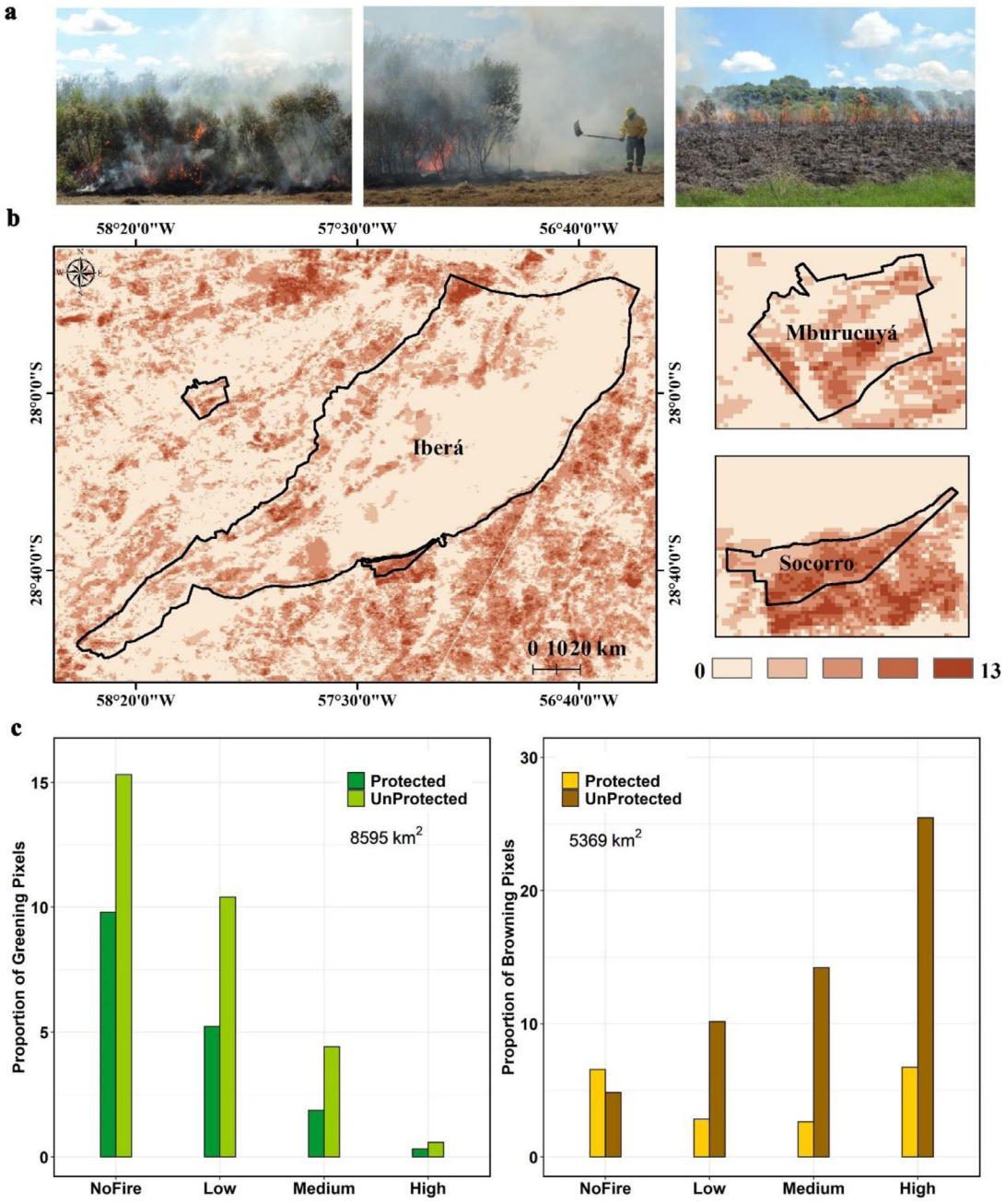

Fig. 6. Greening and browning distribution along fire frequency and land protection status (protected and unprotected) in Iberá. (a) Photos showing the fire in the protected Mburucuyá Park in 2017 (taken by one of the co-authors). (b) Fire occurrence frequency map observed by MODIS satellite between 2001 and 2018 (considering data availability). (c) Proportions of greening and browning pixels for different fire frequency levels (NoFire: FireFreq = 0; Low: 0 < FireFreq < 2; Medium: 2 ≤ FireFreq ≤ 6;High: FireFreq > 6). The proportion was calculated relative to the total pixels by fire frequency level [i.e., the proportion of greening pixels in protected areas with high fire frequency = (Number of greening pixels in high fire frequency in protected areas) / (total number of pixels in high fire frequency pixels)].

areas might also reduce the capability or need to burn grasslands. Our results showed that unprotected areas continue to experience widespread, frequent fires, which are linked to browning, likely reflecting ecosystem degradation (Abreu et al., 2017). Inside the protected areas, there is more browning in unburnt areas compared to low/medium fire frequency, likely reflecting build-up of senescent herbaceous vegetation due to low levels of herbivory.

The Iberá experienced high inter-annual variation of precipitation and a significant increase in annual temperature in the last two decades, consistent with the fact that the global savanna biome has been experiencing rapid climate changes (Hoegh-Guldberg et al., 2018). The inter-annual weather variation seemed to contribute to the widespread vegetation greening along with intra- and inter- vegetation cover transitions, by increasing vegetation productivity in wet years with longer growing season and decreasing evaporation with more soil moisture in cool years. The positive correlation between overall vegetation greenness and annual precipitation and their anomalies and their change rates suggests that greenness is highly driven by inter-annual weather fluctuations. The relatively higher correlation between vegetation greenness and precipitation than temperature suggests that climate-induced changes in water availability have a strong role in shaping rangeland ecosystem dynamics (Sloat et al., 2018). The correspondence between

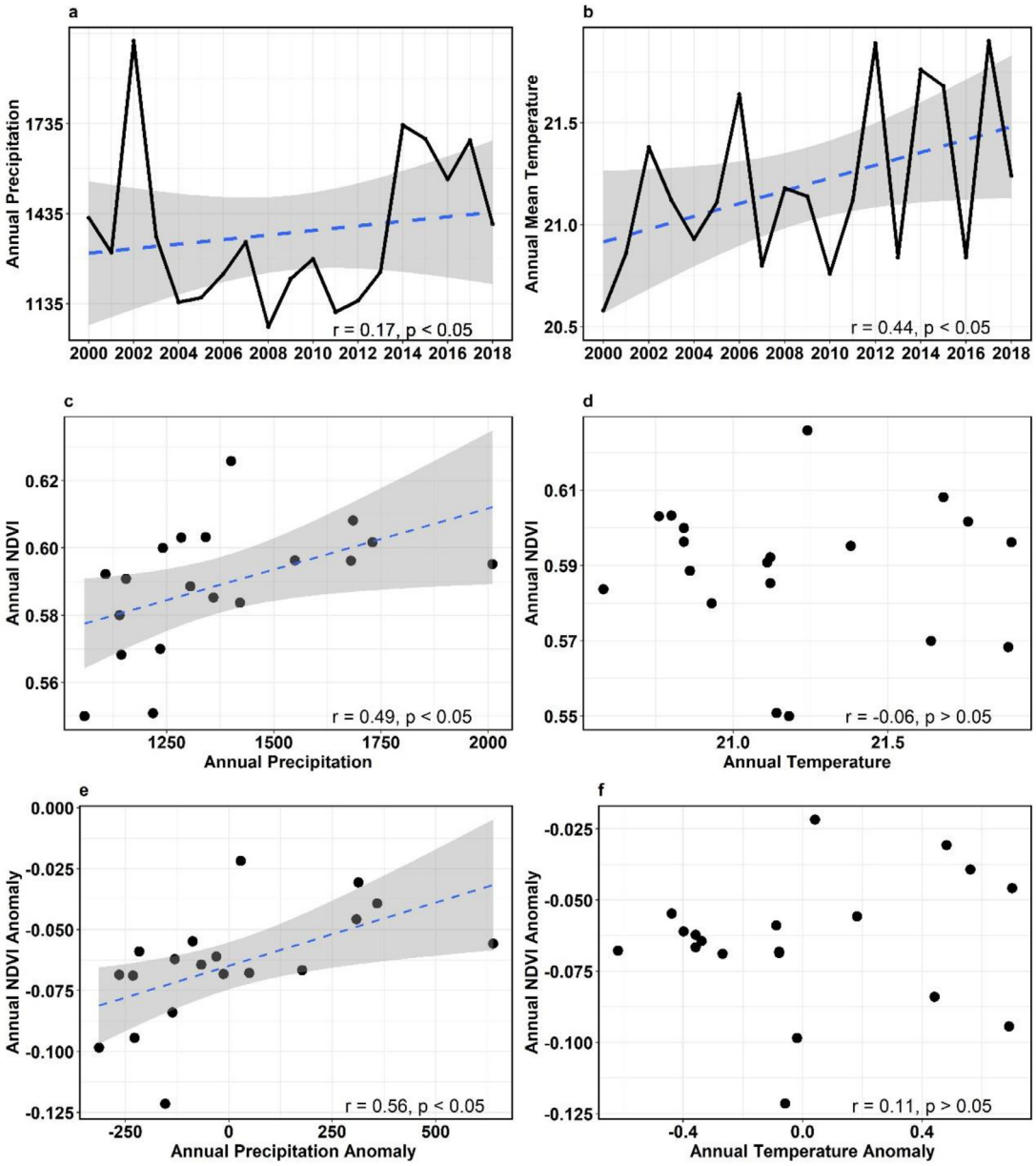

Fig. 7. Inter-annual weather dynamics and associated relationship with NDVI in Iberá between 2000 and 2018. (a) Annual total precipitation. (b) Annual mean temperature. Scatter plot depicts the relationship of annual mean NDVI with (c) annual total precipitation and (d) annual mean temperature. Scatter plot depicts the relationship of annual NDVI anomaly with (e) annual precipitation anomaly and (f) annual temperature anomaly. r represents the Pearson's correlation coefficient at a confidence of 95%. The dashed line represents the fitted line from generalized linear regression.

greening rate of woody and water-related grassy vegetation and inter-annual weather trends suggest that these vegetation types will be highly responsive to climate change, with vegetation growth responding to external climatic factors (Wu et al., 2015). In contrast, the weak correlation between greening rate and inter-annual weather trends for the dry grasslands likely reflect an overwhelming influence of anthropogenic fire regimes and livestock grazing pressure in these areas, as discussed above.

4.3. Implications for ecosystem biodiversity restoration and sustainability

In summary, the Iberá Wetland region has experienced an overall greening trend in the last decades, like many other regions (Piao et al., 2015; Myers-Smith et al., 2020; Li et al., 2020b), with complex land cover dynamics and multiple drivers underlying this pattern. Land management practices including anthropogenic fire regimes, livestock grazing, and conservation protection, emerged to synergistically shape vegetation dynamics in Iberá in interaction with climate dynamics and dam-induced hydrological changes, e.g., annual mean flow and cycle of the neighbouring Paraná river and lake water level (Montroull et al., 2013). We found widespread loss of savannas alongside an increase of wetlands and woody densification partly driven by the expansion of industrial tree plantations and partly by spontaneous woody expansions in terrestrial lands. These woody densification patterns primarily drove greening alongside the expansion of herbaceous wetland vegetation. The implications for biodiversity and society are complex. Given the region's rich savanna biodiversity and the role of livestock in the local culture, the general loss of savannas is clearly negative. The expansion of wetland is positive for aquatic biodiversity, also rich in the region (Zamboni et al., 2017), but still negative for terrestrial biodiversity, and extra problem-

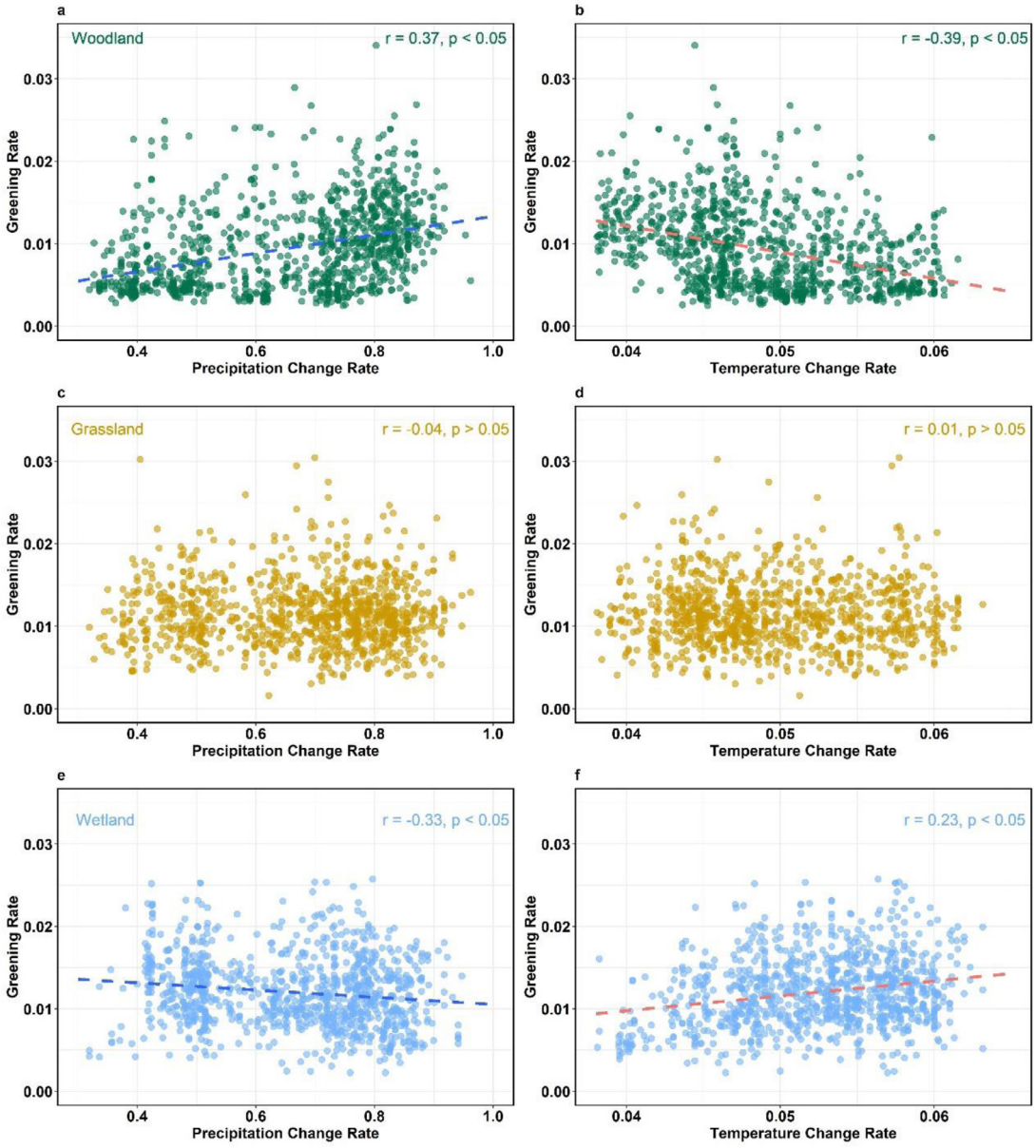

Fig. 8. Relationship between vegetation greening rate and weather trends. Scatter plot between greening rate and annual precipitation change rate (a), (c), (e), and greening rate and annual temperature change rate (b), (d), (f). The vegetation cover types are obtained from the fine-scale reclassified map, including woodland (a, b), grassland (c, d), and herbaceous wetland (e, f). r represents the Pearson's correlation coefficient at a confidence of 95% ($p < 0.05$). The dashed line represents the fitting line from generalized linear regression.

atic in particularly affecting the protected areas. For instance, a significant loss of terrestrial and riparian plant communities was caused by the anthropogenic damming (Bauni et al., 2015). The expansion of industrial tree plantations is clearly negative for biodiversity and local livestock-oriented culture, while the spontaneous woody expansion is likely to have more nuanced effects. A certain level of woody expansion can be seen as constituting recovery and would likely promote biodiversity overall. However, it would become negative if it broadly displaces semi-open and open vegetation, highlighting the importance of ensuring recovery of natural fire and herbivory regimes in the protected areas—in line with the active rewilding activities in parts of Iberá since 2007 (Zamboni et al., 2017) —along with sustainable rangeland management promoting heterogeneous vegetation elsewhere. Our study highlights the need to carefully assess the nature of observed general greening patterns and avoid simplistic interpretations.

5. Conclusion

As the most dominant ice-free land cover, rangelands play a critical role in global environmental changes by contributing to multiple ecological processes across spatial and temporal scales and responding to complex, interacting natural and anthropogenic drivers. There are widespread reports of greening in rangelands globally (Archer et al., 2017; Devine et al., 2017; Li et al., 2020b), with a relatively poor understanding of the drivers and the ecological and social consequences (Li et al., 2020b). The present study addressed the need to understand the complexity behind the reported greening trends, notably whether they represented environmental recovery or degradation based on the case of the highly heterogeneous Iberá Wetlands region in South America. It showcases how the high complexity behind the observed global greening trends can be unpacked and, further highlights the importance

of doing so, as the greening may not necessarily reflect ecosystem recovery, but can also result from land use intensification and associated loss of natural habitats. This is clearly seen here from the strong contribution of industrial tree plantations to the overall greening trend, i.e., a development that represents a threat to both the biodiversity and the livestock-oriented culture in this region. Hereby, our study highlights how detailed remote sensing-based analysis at the landscape level can be used to critically assess the drivers and the implications of the global greening trend. Many of the results of our study were obtained using diverse sources of satellite remote sensing products with a strong support from local collaborators for interpretation of the results. However, we would suggest that future research should consider additional field-based measurements on the vegetation structure and coverage into account. Spontaneous vegetation dynamics, partly involving spontaneous woody expansion, also contribute to the greening trend and have more nuanced implications (Fernandes et al., 2016; Guido et al., 2017; Bond et al., 2019). Notably, such natural woody expansion has a positive potential for biodiversity and ecosystem services, but can become negative in this natural savanna region if expansions develop on a too broad scale (Guido et al., 2017), highlighting the importance of ensuring recovery of natural fire and herbivory regimes in protected areas along with sustainable rangeland management elsewhere.

Data availability

The time-series MODIS NDVI and land cover products, and climate data are open-access in Google Earth Engine (https://earthengine.google.com/datasets/). The final fine-scale land cover map of this study is available from the corresponding author upon reasonable request.

Declaration of Competing Interest

The authors declare no conflict of interest.

Acknowledgements

This work was supported by Troels Myndel Petersens Botanisk Taxonomiske Forskningsfond, the Carlsberg Foundation (Semper Ardens project MegaPast2Future, Grant CF16-000), VILLUM FONDEN (VILLUM Investigator project, Grant 16549), the Youth Innovation Promotion Association CAS (Grant 2018084), H2020 Marie Skłodowska-Curie Actions (Grant 840865), National Natural Science Foundation of China (Grant 41701392, Grant 41871347), Major State Basic Research Development Program of China (Grant 2013CB733405), the Strategic Priority Research Program of the Chinese Academy of Sciences (Grant XDA19030404). We are very thankful for the constructive feedback from Talía Zamboni and Sofia Heinonen in Fundación Rewilding Argentina.

Supplementary materials

Supplementary material associated with this article can be found, in the online version, at doi:10.1016/j.geosus.2020.12.002.

References

Abatzoglou, J.T., Dobrowski, S.Z., Parks, S.A., Hegewisch, K.C., 2018. TerraClimate, a high-resolution global dataset of monthly climate and climatic water balance from 1958–2015. Sci. Data 5, 170191.

Abreu, R.C., Hoffmann, W.A., Vasconcelos, H.L., Pilon, N.A., Rossatto, D.R., Durigan, G., 2017. The biodiversity cost of carbon sequestration in tropical savanna. Sci. Adv. 3 (8), e1701284.

Anadón, J.D., Sala, O.E., Turner, B., Bennett, E.M., 2014. Effect of woody-plant encroachment on livestock production in North and South America. P. Natl. Acad. Sci. USA 111 (35), 12948–12953.

Archer, S.R., Andersen, E.M., Predick, K.I., Schwinning, S., Steidl, R.J., Woods, S.R., 2017. Woody plant encroachment: Causes and consequences. In: Briske, D.D. (Ed.), Rangeland Systems. Springer, pp. 25–84.

Bauni, V., Schivo, F., Capmourteres, V., Homberg, M., 2015. Ecosystem loss assessment following hydroelectric dam flooding: The case of Yacyretá, Argentina. Remote Sensing Applications: Society and Environment 1, 50–60.

Beckage, B., Bucini, G., Gross, L.J., Platt, W.J., Higgins, S.I., Fowler, N.L., Slocum, M.G., Farrior, C., 2019. Water limitation, fire, and savanna persistence: A conceptual model. In: Scogings, P.F., Sankaran, M. (Eds.), Savanna Woody Plants and Large Herbivores, pp. 643–659.

Bernardi, R.E., Holmgren, M., Arim, M., Scheffer, M., 2016. Why are forests so scarce in subtropical South America? The shaping roles of climate, fire and livestock. Forest Ecol. Manag. 363, 212–217.

Bhola, N., Ogutu, J.O., Said, M.Y., Piepho, H.P., Olff, H., 2012. The distribution of large herbivore hotspots in relation to environmental and anthropogenic correlates in the Mara region of Kenya. J. Anim. Ecol. 81 (6), 1268–1287.

Blanco, D.E., Parera, A.F., Acerbi, M. , 2003. La inundación silenciosa. El aumento de las aguas en los Esteros del Ibera: La nueva amenaza de la represa Yacyreta. Version ampliada y actualizada. Fundacion Vida Silvestre Argentina. Buenos Aires 56. (in Spain)

Bond, W.J., Midgley, G.F., 2000. A proposed CO_2-controlled mechanism of woody plant invasion in grasslands and savannas. Global Change Biol. 6 (8), 865–869.

Bond, W.J., Parr, C.L., 2010. Beyond the forest edge: Ecology, diversity and conservation of the grassy biomes. Biol. Conserv. 143 (10), 2395–2404.

Bond, W.J., Stevens, N., Midgley, G.F., Lehmann, C.E.R., 2019. The trouble with trees: Afforestation plans for Africa. Trends Ecol. Evol. 34 (11), 963–965.

Brandt, M., Rasmussen, K., Peñuelas, J., Tian, F., Schurgers, G., Verger, A., Mertz, O., Palmer, J.R., Fensholt, R., 2017. Human population growth offsets climate-driven increase in woody vegetation in sub-Saharan Africa. Nat. Ecol. Evol. 1 (4), 0081.

Buchhorn, M., Smets, B., Bertels, L., Lesiv, M., Tsendbazar, N., Herold, M., Fritz, S., 2019. Copernicus Global Land Service: Land Cover 100m: Epoch 2015: Globe. Version V2. 0.2.

Buitenwerf, R., Bond, W., Stevens, N., Trollope, W., 2012. Increased tree densities in South African savannas: >50 years of data suggests CO_2 as a driver. Global Change Biol. 18 (2), 675–684.

Buitenwerf, R., Sandel, B., Normand, S., Mimet, A., Svenning, J.C., 2018. Land-surface greening suggests vigorous woody regrowth throughout European semi-natural vegetation. Global Change Biol. 24 (12), 5789–5801.

Cabral, A., De Miguel, J., Rescia, A., Schmitz, M., Pineda, F., 2003. Shrub encroachment in Argentinean savannas. J. Veg. Sci. 14 (2), 145–152.

Canziani, G.A., Ferrati, R.M., Rossi, C., Ruiz-Moreno, D., 2006. The influence of climate and dam construction on the Ibera wetlands. Argentina. Reg. Environ. Change 6 (4), 181–191.

Chen, C., Park, T., Wang, X., Piao, S., Xu, B., Chaturvedi, R.K., Fuchs, R., Brovkin, V., Ciais, P., Fensholt, R., Tømmervik, H., Bala, G., Zhu, Z., Nemani, R.R., Myneni, R.B., 2019. China and India lead in greening of the world through land-use management. Nature Sustain. 2 (2), 122–129.

Conradi, T., 2018. Woody encroachment in African savannas: Towards attribution to multiple drivers and a mechanistic model. J. Biogeogr. 45 (6), 1231–1233.

Daskin, J.H., Stalmans, M., Pringle, R.M., 2016. Ecological legacies of civil war: 35-year increase in savanna tree cover following wholesale large-mammal declines. J. Ecol. 104 (1), 79–89.

de Jong, R., de Bruin, S., de Wit, A., Schaepman, M.E., Dent, D.L., 2011. Analysis of monotonic greening and browning trends from global NDVI time-series. Remote Sens. Environ. 115 (2), 692–702.

Devine, A.P., McDonald, R.A., Quaife, T., Maclean, I.M., 2017. Determinants of woody encroachment and cover in African savannas. Oecologia 183 (4), 939–951.

Durigan, G., Ratter, J.A., 2016. The need for a consistent fire policy for Cerrado conservation. J. Appl. Ecol. 53 (1), 11–15.

Eddy, I.M.S., Gergel, S.E., Coops, N.C., Henebry, G.M., Levine, J., Zerriffi, H., Shibkov, E., 2017. Integrating remote sensing and local ecological knowledge to monitor rangeland dynamics. Ecol. Indic. 82, 106–116.

Fagan, M.E., 2020. A lesson unlearned? Underestimating tree cover in dryland biases global restoration maps. Global Change Biol. 26 (9), 4679–4690.

Feng, X., Fu, B., Piao, S., Wang, S., Ciais, P., Zeng, Z., Lü, Y., Zeng, Y., Li, Y., Jiang, X., Wu, B., 2016. Revegetation in China's Loess Plateau is approaching sustainable water resource limits. Nat. Cl. Change 6 (11), 1019–1022.

Fernandes, G.W., Coelho, M.S., Machado, R.B., Ferreira, M.E., Aguiar, L.d.S., Dirzo, R., Scariot, A., Lopes, C.R., 2016. Afforestation of savannas: An impending ecological disaster. Natureza & Conservacao 14 (2), 146–151.

Forkel, M., Carvalhais, N., Rödenbeck, C., Keeling, R., Heimann, M., Thonicke, K., Zaehle, S., Reichstein, M., 2016. Enhanced seasonal CO2 exchange caused by amplified plant productivity in northern ecosystems. Science 351 (6274), 696–699.

Fuhlendorf, S.D., Engle, D.M., 2001. Restoring heterogeneity on rangelands: Ecosystem management based on evolutionary grazing patterns. BioScience 51 (8), 625–632.

Fuhlendorf, S.D., Smeins, F.E., 1999. Scaling effects of grazing in a semi-arid grassland. J. Veg. Sci. 10 (5), 731–738.

Funk, C.C., Peterson, P.J., Landsfeld, M.F., Pedreros, D.H., Verdin, J.P., Rowland, J.D., Romero, B.E., Husak, G.J., Michaelsen, J.C., Verdin, A.P., 2014. A quasi-global precipitation time series for drought monitoring. US Geological Survey.

García Criado, M., Myers-Smith, I.H., Bjorkman, A.D., Lehmann, C.E., Stevens, N., 2020. Woody plant encroachment intensifies under climate change across tundra and savanna biomes. Global Ecol. Biogeogr. 29 (5), 925–943.

Giglio, L., Loboda, T., Roy, D.P., Quayle, B., Justice, C.O., 2009. An active-fire based burned area mapping algorithm for the MODIS sensor. Remote Sens. Environ. 113 (2), 408–420.

Godde, C.M., Garnett, T., Thornton, P.K., Ash, A.J., Herrero, M., 2018. Grazing systems expansion and intensification: Drivers, dynamics, and trade-offs. Glob. Food Secur. 16, 93–105.

González-Roglich, M., Swenson, J.J., Villarreal, D., Jobbágy, E.G., Jackson, R.B., 2015. Woody plant-cover dynamics in argentine savannas from the 1880s to 2000s: The interplay of encroachment and agriculture conversion at varying scales. Ecosystems 18 (3), 481–492.
Guido, A., Salengue, E., Dresseno, A., 2017. Effect of shrub encroachment on vegetation communities in Brazilian forest-grassland mosaics. Perspect. Ecol. Conser. 15 (1), 52–55.
Hegerl, G.C., Hoegh-Guldberg, O., Casassa, G., Hoerling, M.P., Kovats, R., Parmesan, C., Pierce, D.W., Stott, P.A., 2010. Good practice guidance paper on detection and attribution related to anthropogenic climate change. Meeting Report of the Intergovernmental Panel on Climate Change Expert Meeting on Detection and Attribution of Anthropogenic Climate Change. IPCC Working Group I Technical Support Unit, Bern.
Hoegh-Guldberg, O., Jacob, D., Bindi, M., Brown, S., Camilloni, I., Diedhiou, A., Djalante, R., Ebi, K., Engelbrecht, F., Guiot, J., 2018. Impacts of 1.5°C global warming on natural and human systems. Global warming of 1.5°C. An IPCC Special Report.
Holechek, J.L., de Souza Gomes, H., Molinar, F., Galt, D., 1998. Grazing intensity: Critique and approach. Rangelands 20 (5), 15–18.
Holgerson, M.A., Raymond, P.A., 2016. Large contribution to inland water CO_2 and CH_4 emissions from very small ponds. Nature Geosci. 9 (3), 222–226.
Holl, K.D., Brancalion, P.H.S., 2020. Tree planting is not a simple solution. Science 368 (6491), 580–581.
Kissling, W.D., Carl, G., 2008. Spatial autocorrelation and the selection of simultaneous autoregressive models. Global Ecol. Biogeogr. 17 (1), 59–71.
Kulmatiski, A., Beard, K.H., 2013. Woody plant encroachment facilitated by increased precipitation intensity. Nat. Clim. Change 3 (9), 833–837.
Kunst, C., 2011. Ecología y uso del fuego en la región chaqueña Argentina. Boletín Informativo CIDEU (10) 81–105.
Li, W., Buitenwerf, R., Munk, M., Amoke, I., Bøcher, P.K., Svenning, J.C., 2020a. Accelerating savanna degradation threatens the Maasai Mara socio-ecological system. Global Environ. Chang. 60, 102030.
Li, W., Buitenwerf, R., Munk, M., Bøcher, P.K., Svenning, J.C., 2020b. Deep-learning based high-resolution mapping shows woody vegetation densification in greater Maasai Mara ecosystem. Remote Sens. Environ. 247, 111953.
Lunt, I.D., Winsemius, L.M., McDonald, S.P., Morgan, J.W., Dehaan, R.L., 2010. How widespread is woody plant encroachment in temperate Australia? Changes in woody vegetation cover in lowland woodland and coastal ecosystems in Victoria from 1989 to 2005. J. Biogeogr. 37 (4), 722–732.
Macias-Fauria, M., Forbes, B.C., Zetterberg, P., Kumpula, T., 2012. Eurasian Arctic greening reveals teleconnections and the potential for structurally novel ecosystems. Nat. Clim. Change 2 (8), 613–618.
Macias, D., Mazía, N., Jacobo, E., 2014. Grazing and neighborhood interactions limit woody encroachment in wet subtropical savannas. Basic Appl. Ecol. 15 (8), 661–668.
Malhi, Y., Roberts, J.T., Betts, R.A., Killeen, T.J., Li, W., Nobre, C.A., 2008. Climate change, deforestation, and the fate of the Amazon. Science 319 (5860), 169–172.
Mann, H.B., 1945. Nonparametric tests against trend. Econometrica 13 (3), 245–259.
McCollum III, F.T., Gillen, R.L., Karges, B.R., Hodges, M.E., 1999. Stocker cattle response to grazing management in tallgrass prairie. J. Range. Manag. 52 (2), 120–126.
Mishra, N.B., Mainali, K.P., 2017. Greening and browning of the Himalaya: Spatial patterns and the role of climatic change and human drivers. Sci. Total Environ. 587, 326–339.
Montroull, N.B., Saurral, R.I., Camilloni, I.A., Grimson, R., Vasquez, P., 2013. Assessment of climate change on the future water levels of the Iberá wetlands, Argentina, during the twenty-first century. Int. J. River Basin Manage. 11 (4), 401–410.
Myers-Smith, I.H., Kerby, J.T., Phoenix, G.K., Bjerke, J.W., Epstein, H.E., Assmann, J.J., John, C., Andreu-Hayles, L., Angers-Blondin, S., Beck, P.S.A., Berner, L.T., Bhatt, U.S., Bjorkman, A.D., Blok, D., Bryn, A., Christiansen, C.T., Cornelissen, J.H.C., Cunliffe, A.M., Elmendorf, S.C., Forbes, B.C., Goetz, S.J., Hollister, R.D., de Jong, R., Loranty, M.M., Macias-Fauria, M., Maseyk, K., Normand, S., Olofsson, J., Parker, T.C., Parmentier, F.-J.W., Post, E., Schaepman-Strub, G., Stordal, F., Sullivan, P.F., Thomas, H.J.D., Tømmervik, H., Treharne, R., Tweedie, C.E., Walker, D.A., Wilmking, M., Wipf, S., 2020. Complexity revealed in the greening of the Arctic. Nat. Clim. Change 10 (2), 106–117.
Neiff, J., de Neiff, A.P., 2006. Situación ambiental en la ecorregión Iberá. La situación ambiental Argentina 2005 (01), 177–184.
O'Connor, T.G., Puttick, J.R., Hoffman, M.T., 2014. Bush encroachment in southern Africa: Changes and causes. Afr. J. Range. For. Sci. 31 (2), 67–88.
Patten, R.S., Ellis, J.E., 1995. Patterns of species and community distributions related to environmental gradients in an arid tropical ecosystem. Vegetatio 117 (1), 69–79.
Pearson, R.G., Phillips, S.J., Loranty, M.M., Beck, P.S., Damoulas, T., Knight, S.J., Goetz, S.J., 2013. Shifts in Arctic vegetation and associated feedbacks under climate change. Nat. Clim. Change 3 (7), 673–677.
Pekel, J.F., Cottam, A., Gorelick, N., Belward, A.S., 2016. High-resolution mapping of global surface water and its long-term changes. Nature 540 (7633), 418–422.
Piao, S., Wang, X., Park, T., Chen, C., Lian, X., He, Y., Bjerke, J.W., Chen, A., Ciais, P., Tømmervik, H., Nemani, R.R., Myneni, R.B., 2020. Characteristics, drivers and feedbacks of global greening. Nat. Rev. Earth Environ. 1, 14–27.
Piao, S., Yin, G., Tan, J., Cheng, L., Huang, M., Li, Y., Liu, R., Mao, J., Myneni, R.B., Peng, S., Poulter, B., Shi, X., Xiao, Z., Zeng, N., Zeng, Z., Wang, Y., 2015. Detection and attribution of vegetation greening trend in China over the last 30 years. Global Change Biol. 21 (4), 1601–1609.
Putuhena, W.M., Cordery, I., 2000. Some hydrological effects of changing forest cover from eucalypts to Pinus radiata. Agr. Forest Meteorol. 100 (1), 59–72.
Rangel, T.F., Diniz-Filho, J.A.F., Bini, L.M., 2010. SAM: A comprehensive application for spatial analysis in macroecology. Ecography 33 (1), 46–50.
Sandel, B., Svenning, J.C., 2013. Human impacts drive a global topographic signature in tree cover. Nat. Commun. 4, 2474.
Sloat, L.L., Gerber, J.S., Samberg, L.H., Smith, W.K., Herrero, M., Ferreira, L.G., Godde, C.M., West, P.C., 2018. Increasing importance of precipitation variability on global livestock grazing lands. Nat. Clim. Change 8 (3), 214–218.
Soares-Filho, B.S., Rodrigues, H.O., Costa, W., 2009. Modeling environmental dynamics with Dinamica EGO. In: Centro de Sensoriamento Remoto. Universidade Federal de Minas Gerais, Belo Horizonte, Minas Gerais, p. 115.
Stevens, N., Erasmus, B., Archibald, S., Bond, W., 2016a. Woody encroachment over 70 years in South African savannahs: Overgrazing, global change or extinction aftershock? Philos. T. R. Soc. B 371, 20150437.
Stevens, N., Lehmann, C.E.R., Murphy, B.P., Durigan, G., 2016b. Savanna woody encroachment is widespread across three continents. Global Change Biol. 23 (1), 235–244.
Stow, D.A., Hope, A., McGuire, D., Verbyla, D., Gamon, J., Huemmrich, F., Houston, S., Racine, C., Sturm, M., Tape, K., 2004. Remote sensing of vegetation and land-cover change in Arctic Tundra Ecosystems. Remote Sens. Environ. 89 (3), 281–308.
Tsegaye, D., Moe, S.R., Vedeld, P., Aynekulu, E., 2010. Land-use/cover dynamics in Northern Afar rangelands, Ethiopia. Agr. Ecos. Environ. 139 (1–2), 174–180.
Vörösmarty, C.J., Green, P., Salisbury, J., Lammers, R.B., 2000. Global water resources: vulnerability from cimate change and population growth. Science 289 (5477), 284–288.
Veldman, J.W., Overbeck, G., Negreiros, D., Mahy, G., Le Stradic, S., Fernandes, G.W., Durigan, G., Buisson, E., Putz, F.E., Bond, W.J., 2015. Tyranny of trees in grassy biomes. Science 347 (6221), 484–485.
Venter, Z.S., Cramer, M.D., Hawkins, H.J., 2018. Drivers of woody plant encroachment over Africa. Nat. Commun. 9, 2272.
Vickers, H., Høgda, K.A., Solbø, S., Karlsen, S.R., Tømmervik, H., Aanes, R., Hansen, B.B., 2016. Changes in greening in the high Arctic: Insights from a 30 year AVHRR max NDVI datasIet for Svalbard. Environ. Res. Lett. 11 (10), 105004.
Walker, B., Holling, C.S., Carpenter, S.R., Kinzig, A.P., 2004. Resilience, Adaptability and Transformability in Social-ecological Systems. Ecol. Soc. 9 (2), 5.
Wang, F., Shao, W., Yu, H., Kan, G., He, X., Zhang, D., Ren, M., Wang, G., 2020. Re-evaluation of the Power of the Mann-Kendall Test for Detecting Monotonic Trends in Hydrometeorological Time Series. Front. Earth Sci. 8, 14.
Wei, F., Wang, S., Fu, B., Brandt, M., Pan, N., Wang, C., Fensholt, R., 2020. Nonlinear dynamics of fires in Africa over recent decades controlled by precipitation. Global Change Biol. 26 (8), 4495–4505.
Wu, D., Zhao, X., Liang, S., Zhou, T., Huang, K., Tang, B., Zhao, W., 2015. Time-lag effects of global vegetation responses to climate change. Global Change Biol. 21 (9), 3520–3531.
Zamboni, T., Di Martino, S., Jiménez-Pérez, I., 2017. A review of a multispecies reintroduction to restore a large ecosystem: The Iberá Rewilding Program (Argentina). Perspect. Ecol. Conser. 15 (4), 248–256.
Zeng, Y., Yang, X., Fang, N., Shi, Z., 2020. Large-scale afforestation significantly increases permanent surface water in China's vegetation restoration regions. Agr. Forest Meteorol. 290, 108001.
Zhang, W., Brandt, M., Penuelas, J., Guichard, F., Tong, X., Tian, F., Fensholt, R., 2019. Ecosystem structural changes controlled by altered rainfall climatology in tropical savannas. Nat. Commun. 10, 671.
Zhu, Z., Piao, S., Myneni, R.B., Huang, M., Zeng, Z., Canadell, J.G., Ciais, P., Sitch, S., Friedlingstein, P., Arneth, A., 2016. Greening of the Earth and its drivers. Nat. Clim. Change 6 (8), 791–795.